Heliyon 10 (2024) e28904

Contents lists available at ScienceDirect

Heliyon

journal homepage: www.cell.com/heliyon

Research article

Mechanical properties and microstructure of brick aggregate concrete with raw fly ash as a partial replacement of cement

Md. Nazrul Islam [a], Md. Abu Noaman [b,*], Khandaker Saiful Islam [b], Mohammad Abu Hanif [b]

[a] Department of Civil Engineering, Dhaka University of Engineering & Technology, Gazipur, 1707, Bangladesh
[b] Dhaka University of Engineering & Technology, Gazipur, 1707, Bangladesh

ARTICLE INFO

Keywords:
Brick aggregate concrete
Raw fly ash
Mechanical properties
Microstructure

ABSTRACT

In response to environmental concerns, researchers explore fly ash as a cement replacement material, and crushed bricks as a cost-effective and load-reducing aggregate, particularly where stone chips are scarce. Therefore, this study investigates the mechanical properties and microstructure of brick aggregate concrete (BAC) with raw fly ash (FA) as a partial replacement of cement. The research involved casting raw FA based BAC (FBAC) cylinders (100 mm diameter and 200 mm height) and prism (100 × 100 × 500 mm) with varying levels of FA (0–25%) using a constant mix proportion by volume of 1:1.5:3 (cement : fine aggregate : coarse aggregate) with a water to binder (w/b) ratio of 0.50 and three curing ages (7, 28, and 90 days). Tests for mechanical properties, including compressive strength, split tensile strength, flexural strength, modulus of elasticity, and Poisson's ratio were conducted to assess the behavior of FBAC, and microstructure were then investigated at 28 days. The results indicated that increasing the FA content up to 15% led to gradual improvement in compressive strength and tensile strength values. At 28 days, the highest values of compressive strength and split tensile strength were observed at 10% FA, with 7.9% and 14.2% increase, respectively, compared to the control concrete. However, the flexural strength of FBAC decreased gradually with cement replacement. On the other hand, modulus of elasticity and Poisson's ratio increased gradually up to 20% and 25% cement replacement, respectively. Up to 15% FA enhanced a more uniform and compact microstructure than that of control concrete. Several equations have been developed to express relationship between compressive strength and other mechanical properties of FBAC. Hence, up to 15% raw FA as a partial replacement of cement improved the mechanical properties and microstructure of BAC.

1. Introduction

Fly ash (FA) is a by-product of burning pulverized coal in a power station. In Bangladesh, the annual production of FA is about 500 million tons, but only about 20% is utilized in the concrete industry [1]. The rest of this ash is used to be dumped as waste in ponds or landfills and so on, which leads to environmental pollution [2]. Thus, recycling this ash is an urgent issue. In 2021, global CO_2

* Corresponding author.
E-mail addresses: nazrul2100@duet.ac.bd (Md.N. Islam), noaman_ce07@yahoo.com (Md.A. Noaman), belbpl87@gmail.com (K.S. Islam), engrhanif80@gmail.com (M.A. Hanif).

https://doi.org/10.1016/j.heliyon.2024.e28904
Received 31 January 2024; Received in revised form 15 March 2024; Accepted 26 March 2024
Available online 30 March 2024
2405-8440/

emissions surged by 5%, primarily due to a 60% increase in coal demand, as reported by Nayak et al. [3] and the International Energy Agency [4]. The cement sector, a substantial contributor, stands responsible for 7% of total global CO_2 emissions [5], emits approximately 0.5–0.9 kg of CO_2 per kg of cement production, leading to annual emissions of around 3.24 billion tonnes and this trend will continue until 2050 [6]. As a consequence, a number of researchers [7–11] utilized FA in concrete in order to reduce cement content. This step reduces both energy consumption and CO_2 emissions from the production of cement. Several researchers [8,12] have already used FA as an ordinary Portland cement (OPC) replacement material in concrete construction as it is rich in silica. Li and Wu [13] have demonstrated that the size of FA affects the strength of masonry mortars and FA retained less than 5% by weight on sieve No. 325 (45 μm) acts as good pozzolana [14]. Toutanji et al. [15] reported that the strength of concrete increases with the fineness, types and amount of FA content. The authors [15] also claimed that Class C ash indicates higher earlier strength than Class F ash. On the other hand, coarse aggregate plays a vital role in the strength of concrete [16]. Recently, crushed brick has become more popular in South Asia as a coarse aggregate in making concrete due to the scarcity of stone aggregate [16–18]. Several studies have already been made to evaluate the strength of concrete with FA in stone aggregate concrete [19,20]. Papadakis and Tsimas [21] reported that the strength of FA mixed concrete is reduced at an early age, and the strength becomes higher at 90 days. In contrast, Babu and Rao [22] reported that the concretes with 10% FA exhibited higher strength at early and long ages. Concrete with 10% FA shows a homogeneous and dense microstructure [10]. The pore size in concrete reduces gradually with FA content up to 30% by filling the gaps between the aggregates [9,11]. Although many attempts have been made to use FA in stone aggregate concrete [9–11,15,21], none of these researchers considered crushed brick as coarse aggregate including raw FA. However, a great number of researchers [16,23–28] have studied the properties of brick aggregate concrete (BAC), but, to the best of the authors' knowledge, only a few researchers [7] used FA as a partial replacement of cement in concrete, which was made of 50% crushed brick plus 50% stone chips as coarse aggregate. However, these researches [7,9–11,15,16,21,23–28] have not investigated concrete using raw FA as a partial replacement of cement with 100% brick chips as coarse aggregate. In addition, none of these studies [7,9–11,15,16,21,23–28] have assessed the relationship between compressive strength and other mechanical properties (such as split tensile strength, flexural strength, and modulus of elasticity) of BAC containing raw FA as a partial replacement of cement at a constant mix proportion of 1:1.5:3 (cement : fine aggregate : coarse aggregate) and a water-to-binder (w/b) ratio of 0.50. Addressing the above-mentioned research gaps, this study investigated the mechanical properties and microstructure of FBAC (raw FA based BAC).

2. Materials and methodology

2.1. Test on materials

A local company in Bangladesh supplied well-burnt, irregular, reddish colored bricks called "picked bricks" for experiment. These bricks were crushed manually and screened to a maximum size of 19 mm. Local river sand, known as fine aggregate, was used to fill the spaces left by the coarse aggregate. A number of tests were conducted in accordance with ASTM standards to know the physical characteristics of the coarse and fine aggregates, as presented in Table 1.

The raw fly ash and ordinary Portland cement (OPC) used in the experiment was obtained from a local company. The fineness of the raw FA and OPC was tested using an ASTM 75 μm (No. 200) sieve, while their physical properties, such as specific gravity and density, were evaluated using BS test methods, as indicated in Table 2. ASTM standard tests were performed on OPC (ASTM Type I) to measure its physical and mechanical properties, as presented in Table 2. The morphology of raw FA was scrutinized by Scanning Electron Microscope (SEM) test. The chemical component of the raw FA and OPC was assessed by X-ray fluorescence analysis, and the electric muffle furnace was used to evaluate the loss on ignition (LOI) of FA. The results are presented in Table 3. The X-ray diffraction (XRD) analysis was conducted using an XRD machine, and the data were examined using MATCH software (version 3.0). The concrete mixing and curing process was done using laboratory drinking water.

Table 1
Physical properties of coarse and fine aggregates.

Properties	Test standard	Coarse aggregate (Brick chips)				Fine aggregate (River sand)			
		Present study	Noaman et al. [26]	Rashid et al. [28]	Rashid et al. [27]	Present study	Noaman et al. [26]	Rashid et al. [28]	Rashid et al. [27]
Unit weight (kg/m^3)	ASTM C29 [29]	928	925	903	1088	1202	1386	–	–
Fineness modulus	ASTM C136 [30]	7.22	7.00	7.17	6.97	1.94	2.10	1.62	1.86
Water absorption (%)	ASTM C127 [31]/ASTM C128 [32]	17.50	16.38	16.00	15.80	2.04	1.04	2.04	2.60
Specific gravity (SSD)	ASTM C127 [31]/ASTM C128 [32]	1.97	2.56	2.03	2.10	2.63	2.68	2.65	2.50
Moisture content (%)	ASTM C566 [33]	–	–	–	–	1.78	2.58	–	–

– values are not available.

Table 2
Physical and mechanical properties of OPC and raw FA.

Properties	Test standard	OPC				Raw FA			
		Present study	ASTM C150 [34]	Nanda and Rout [35]	Noaman et al. [16]	Present study	Amin and Abdelsalam [36]	Durán-Herrera et al. [37]	Nanda and Rout [35]
Passing through 75 μm (No. 200) sieve (%)	–	100	–	100	100	70	100	100	97
Color	–	Grey black	–	–	Grey black	Grey	Light grey	–	–
Specific gravity	BS 1377 [38]	3.12	–	3.15	3.11	2.17	2.40	2.38	2.38
Density (kg/m^3)	BS 1377 [38]	1440	–	–	–	1086	–	–	–
Normal consistency (%)	ASTM C187 [39]	28	28–32	–	29	–	–	–	–
Initial setting time (min)	ASTM C191 [40]	105	$\geq$ 45	–	123	–	–	–	–
Final setting time (min)	ASTM C191 [40]	300	$\leq$ 375	–	328	–	–	–	–
3 days compressive strength (MPa)	ASTM C109 [41]	24.16	$\geq$ 12	–	23.44	–	–	–	–
28 days compressive strength (MPa)	ASTM C109 [41]	33.07	$\geq$ 28	48.30	33.72	–	–	–	–

– values are not available.

Table 3
Chemical composition of raw FA and OPC.

Materials	SiO_2	Al_2O_3	Fe_2O_3	K_2O	CaO	TiO_2	MgO	SO_3	Na_2O	LOI	Reference
Raw FA	64.27	22.17	5.06	2.17	1.39	1.06	0.87	–	0.11	2.21	Present study
FA	61.06	28.55	3.15	1.15	1.41	0.35	1.32	1.06	0.71	1.19	Amin and Abdelsalam [36]
FA	62.30	22.00	6.00	1.60	3.40	–	1.00	0.20	0.80	1.60	Durán-Herrera et al. [37]
Class F pozzolana	($SiO_2 + Al_2O_3 + Fe_2O_3$) > 70			–	–	–	–	–	< 3	–	ASTM C618 [42]
OPC	20.40	5.22	3.45	0.46	64.29	–	1.92	2.72	0.45	0.78	Present study
OPC	19.70	6.46	3.66	0.75	62.15	–	2.10	2.51	0.85	1.73	Amin and Abdelsalam [36]
OPC	19.60	4.50	4.00	1.40	58.80	–	1.60	3.00	0.40	6.40	Durán-Herrera et al. [37]
ASTM Type I OPC	–	–	–	–	–	–	< 6	< 3	–	< 3	ASTM C150 [34]

– values are not available.

2.2. *Mix design for concrete specimens*

The mix design and a suitable water-to-binder ratio (w/b = 0.50) for BAC, used in the experiment, were obtained from Noaman et al. [26] and are presented in Table 4. The authors [26] calculated the mix design for 1 m^3 of BAC product, with rice husk ash replacing 0–25% of OPC, using a mix proportion of 1:1.5:3. Noaman et al. [26] employed the absolute volume method to determine the mix design, which was also followed in this experiment.

2.3. *Mixing and slump tests on fresh FBAC*

To maintain mix proportion, all of the materials, including saturated surface dry aggregates, FA, OPC, and water, were put into the mixing machine and mixed for 2–3 minutes. Prior to casting concrete specimens, the workability of fresh concrete was assessed by the slump test, in accordance with ASTM C143 [43]. In this study, raw FA was employed to replace cement in BAC at five different levels

Table 4
Mix design computed for 1 m^3 of FBAC (water-to-binder ratio = 0.50).

Mix designation	Raw FA (%)	OPC (kg)	Raw FA (kg)	Coarse aggregate (kg)	Fine aggregate (kg)	Water (kg)
FBAC0	0	392.73	–	759.27	491.73	196.36
FBAC10	10	353.46	39.27	759.27	491.73	196.36
FBAC15	15	333.82	58.91	759.27	491.73	196.36
FBAC20	20	314.18	78.55	759.27	491.73	196.36
FBAC25	25	294.55	98.18	759.27	491.73	196.36

FBAC0 means BAC containing 0% raw FA.

(0%, 10%, 15%, 20%, and 25% by weight of cement) and the findings were compared to those of the control concrete.

2.4. Casting of FBAC specimens

In this investigation, FBAC specimens were made using steel cylindrical molds (100 × 200 mm) and prism molds (100 × 100 × 500 mm). Each mold was cleaned with a wire brush and its joints were fastened with nut-bolts. The interior and bottom surfaces of the mold were then greased with oil to facilitate the removal of the concrete specimen. The molds were flattened on the floor before casting the concrete specimens. Following the unloading of the mixing machine, the concrete was poured in the mold in three layers and compressed using a tamping bar in accordance with ASTM C31 [44]. All FBAC specimens were kept at room temperature for 24 h. After that time, hardened specimens were removed from the mold. The specimens were then given an identifying mark and placed in water for curing to the desired period.

2.5. Tests on hardened FBAC specimens

Cylindrical specimens were prepared for compressive strength ($f_c^{'}$) test using a compression testing machine after 7, 28, and 90 days of curing, in accordance with ASTM C39 [45]. Unreinforced concrete beams (100 × 100 × 500 mm) were also subjected to flexural strength (f_r) test using a universal testing machine after 28 days of curing, following the ASTM C293 [46]. Additionally, after 28 days of curing, cylindrical specimens were prepared for split tensile strength (f_{sp}), modulus of elasticity (E_c), and Poisson's ratio (μ) tests using a universal testing machine, in accordance with ASTM C496 [47], ASTM C469 [48], and ASTM C469 [48], respectively. For E_c and μ tests, the $f_c^{'}$ was assessed using a universal testing machine, and axial deformation was determined using one dial gauge, while lateral deformation of the cylinder specimens were determined using two dial gauges at mid-height. Three FBAC specimens were tested for each replacement, and their average values were reported.

2.6. Microstructure of FBAC

In this study, Scanning Electron Microscope (SEM) test was conducted to examine the microstructure of FBAC. Concrete (FBAC) cylinders were cast using a mix proportion of 1:1.5:3 and a water-to-binder ratio of 0.50. After 28 days of water curing, the specimens were cut into 10 × 10 mm sizes and polished to reveal a fresh surface for examination under the SEM.

3. Results and discussions

3.1. Properties of materials

Table 1 presents the physical properties of coarse and fine aggregate, which are comparable to those of previous studies [26–28]. Table 2 provides the physical and mechanical properties of OPC and raw FA. These results align closely with previous studies [16, 35–37]. In addition, the OPC used in this study meets the physical and mechanical requirements of ASTM Type I [34]. Fig. 1 displays the morphology of raw FA, indicating that a few particles are spherical in shape and many exhibit elongated, irregular shapes with rough surfaces. Table 3 compares the chemical compositions of FA and OPC with past researches [36,37] and ASTM requirements [34, 42], revealing that 64.27% silica is present in FA, which regulates the continuous hydration process known as the pozzolanic reaction in concrete. On the contrary, CaO in OPC is around 64.29%, which is another ingredient that aids in the pozzolanic reaction. Based on past research and ASTM requirements (Table 3), the FA used in this experiment is confirmed to be Class F pozzolana and the cement is OPC (ASTM Type I).

Furthermore, Fig. 2 illustrates the X-ray diffraction pattern of the FA particle, showing a very sharp peak at about 26.67° (2θ) indicating crystalline SiO_2. This SiO_2 has a trigonal structure with a hexagonal axis and is commonly known as quartz. The presence of

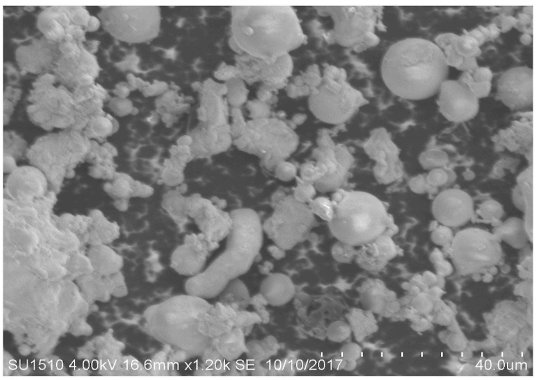

Fig. 1. SEM photograph of raw fly ash.

amorphous silica is indicated by a hump peak between approximately 14° and 30° (2θ). This observation is consistent with previous studies [49,50].

3.2. Workability of fresh FBAC

Fig. 3 illustrates the slump test results of the control BAC (0% FA) and BAC containing FA (10–25%). The slump value of control concrete was 70.0 mm with water-to-binder (w/b) ratio of 0.50. In contrast, the slump values of BAC at all FA replacement levels gradually decreased compared to that of the control concrete. Similar findings were reported by preceding studies [36,51], which demonstrated that increasing FA content in concrete reduced slump values, which means decrease in workability. This is attributed to the dry and irregular shape of FA, which requires more water and increases friction, reducing the flow-ability of concrete [35,52]. According to Fantu et al. [51], the workability of fresh concrete reduces when the inclusion of FA exceeds 10% of the cement. The non-spherical, elongated, irregular shapes and rough surfaces of FA particles (Fig. 1) are deemed to be responsible for reducing the workability of FBAC by increasing the friction between the aggregate and cement paste interface and gradually reducing the ball bearing effect at the interface. Hence, the workability of FBAC decreases with an increase in raw FA content.

3.3. Mechanical properties of FBAC

3.3.1. Compressive strength ($f_c^{'}$)

The compressive strength of FBAC is illustrated in Fig. 4, for 7, 28, and 90 days of curing. The compressive strengths of the control concrete were 20.2 MPa, 23.1 MPa, and 24.3 MPa for 7, 28, and 90 days of curing, respectively. At 7 days, the control concrete achieved 0.2%, 8.5%, 20%, and 23.8% higher strength compared to BAC containing 10%, 15%, 20%, and 25% FA, respectively. This may be due to the dilution effect and delayed pozzolanic action of FA [53–55]. At 28 days, BAC containing 10% and 15% FA achieved 7.9% and 1.8% higher strength compared to control concrete, respectively. At 90 days, BAC with 10% and 15% FA developed 13.7% and 4.2% higher strength, respectively. This improved behavior may be attributed to the pozzolanic and filler effect of FA [53–55]. BAC containing 10% FA showed the maximum strength at 28 and 90 days, possibly due to the ideal replacement of FA in BAC. However, BAC containing higher amount of FA (20% and 25%) showed lower strength at 28 and 90 days. This may be due to the increase in silica (contained in FA) and the gradual reduction of calcium oxide (contained in OPC) in the concrete, leading to unavailability of CaO for pozzolanic reaction. The strength development of concrete containing FA is slow at early ages but shows superior strength at later ages compared to the control concrete [53–55]. Sun et al. [55] used 40% FA in stone aggregate concrete and stated that high-volume FA concrete exhibited lower strength at early ages but higher strength at later ages. This is attributed to the

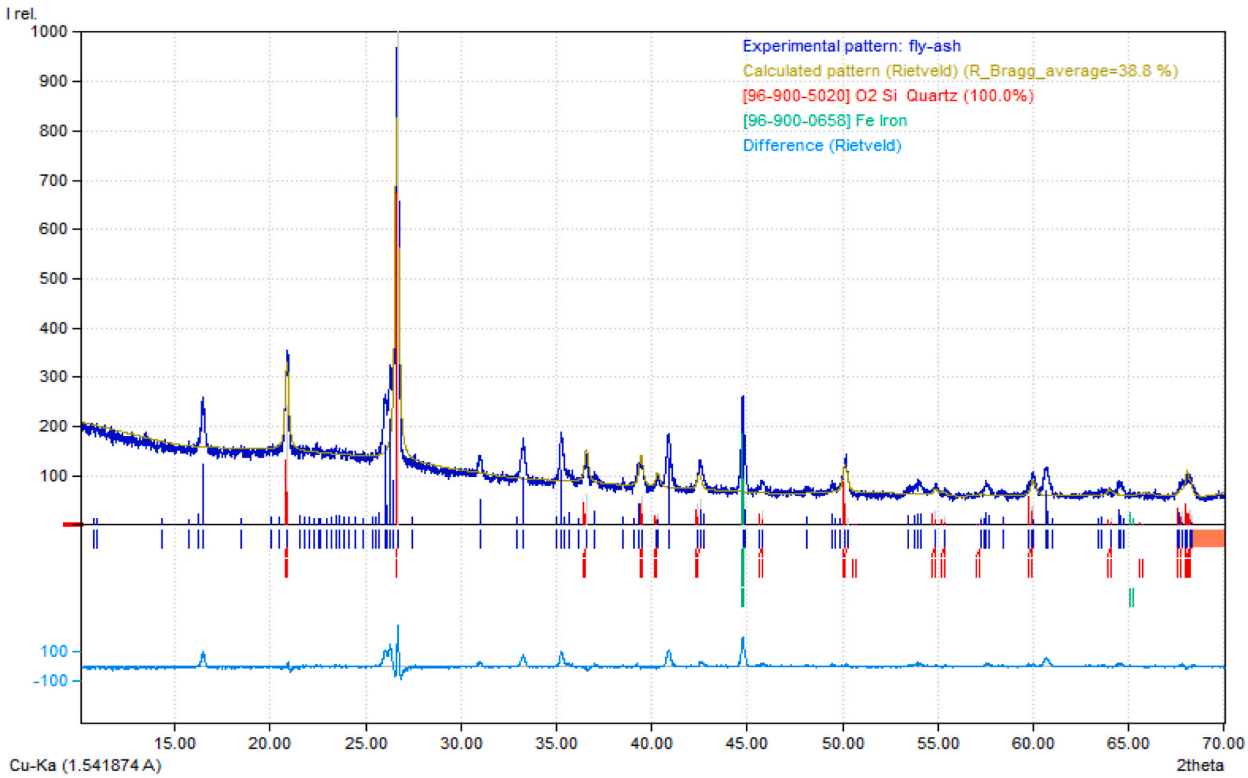

Fig. 2. XRD pattern of raw fly ash.

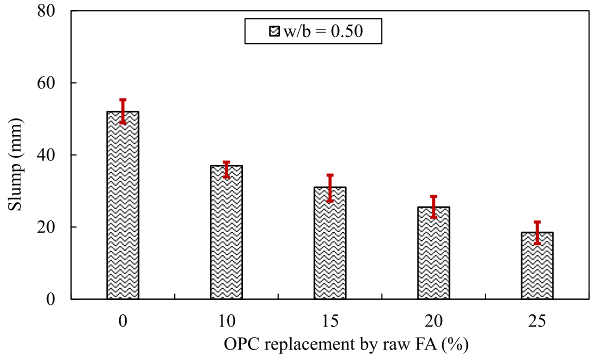

Fig. 3. Slump values of FBAC.

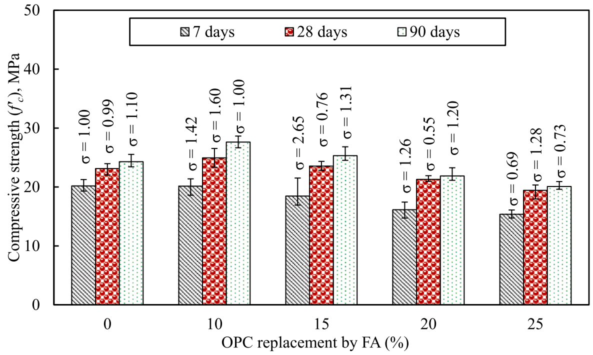

Fig. 4. Compressive strength of FBAC (σ = standard deviation).

pozzolanic properties of FA.

3.3.2. Split tensile strength (f_{sp})

The split tensile strengths of FBAC at 28 days are shown in Fig. 5. The figure demonstrates that the tensile strength of the control concrete was 1.62 MPa. BAC with 10% and 15% FA achieved 14.2% and 8.0% higher strength compared to the control concrete, respectively. Among them, the concrete with 10% FA showed the highest split tensile strength and may be considered the desired limit for tensile strength. Muhit et al. [56] also obtained similar results and stated that the split tensile strength of 10% FA was optimal and increased strength by more than 28%. The tensile strength of BAC increases with the FA content up to 15%, but decreases by 7.4% and 11.7% for 20% and 25% FA replacements, respectively. Therefore, BAC with 15% FA replacement may be the maximum limit for split tensile strength. Siddique [57] observed that the inclusion of 35%, 45%, and 55% FA as a replacement for cement resulted in reductions of 23%, 36%, and 49% in the split tensile strengths of concrete, respectively. Bouzoubaâ et al. [58] stated that the 28-day split tensile strength for FA-mixed concrete was about 3 MPa.

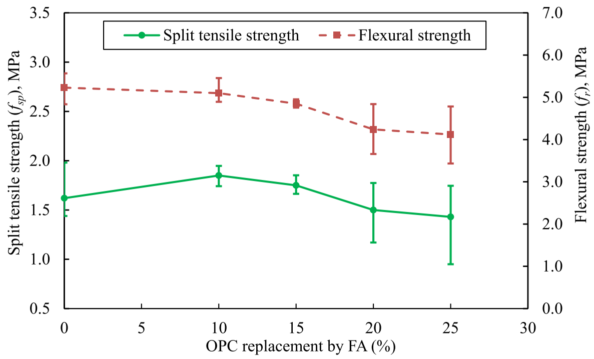

Fig. 5. Split tensile strength and flexural strength of FBAC.

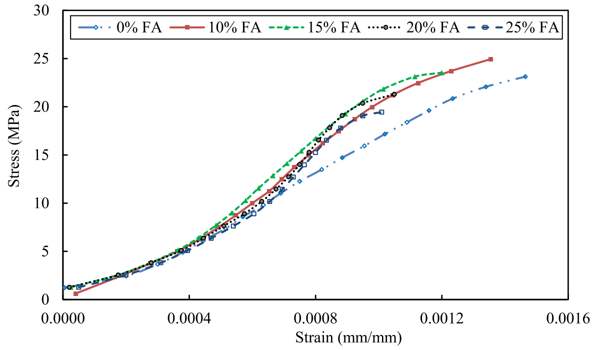

Fig. 6. Relationship between stress and strain of FBAC after 28 days of curing.

3.3.3. *Flexural strength* (f_r)

The 28-day flexural strengths of FA-mixed BAC are also shown in Fig. 5. The figure demonstrates that the flexural strength of the control concrete was 5.23 MPa. The strengths of BAC containing 10%, 15%, 20%, and 25% FA dropped by 2.5%, 7.3%, 18.9%, and 21.2%, respectively. The results also reveal that the flexural strength of FBAC is lower compared to the control concrete. Similar results were obtained by Upadhyay et al. [59]. The authors [59] found that the flexural strength of 10%, 20%, 30%, 40%, and 50% FA concrete decreased by 5.26%, 7.89%, 10.53%, 21.05%, and 42.11%, respectively, compared to the control at 28 days where the w/b ratio was 0.48. Upadhyay et al. [59] hypothesized that this decrease in strength might be caused by the short duration of curing, but at longer ages, the strength might recover. In this study, the flexural strength was lower for 10–25% FA concrete.

3.3.4. *Modulus of elasticity* (E_c)

The relationship between stress and strain of FBAC after 28 days of curing is shown in Fig. 6, and the modulus of elasticity of FBAC is shown in Fig. 7. The secant tangent modulus method (stress at 0.40 $f_c^{'}$), as described by ASTM C469 [48] and Neville [60], was used to determine the modulus of elasticity. The figures reveal that the modulus of elasticity of the control BAC was 15.25 GPa. Brandt [61] noted that the modulus of elasticity for BAC varied from 10 to 30 GPa. The modulus of elasticity of BAC containing 10%, 15%, and 20% FA increased by 9.2%, 12.3%, and 0.6%, respectively. This increase may be attributed to the inclusion of FA, which enhances the elastic properties of concrete. Fig. 7 shows that the modulus of elasticity was higher for all replacement levels (10–20% FA) except 25% replacement compared to the control. For 25% replacement, the modulus of elasticity of FBAC decreased by 6.9% than that of control concrete may be due to the higher replacement. The figure also illustrates that the BAC containing 15% FA exhibits the highest modulus of elasticity among all replacement levels. Durán-Herrera et al. [37] made a similar observation and reported that FA (up to 15%) resulted in an increase in the modulus of elasticity of up to 8%.

3.3.5. *Poisson's ratio (μ)*

The Poisson's ratios of FA-mixed BAC (0%, 10%, 15%, 20%, and 25%) are also shown in Fig. 7. The figure shows that the Poisson's ratio of control BAC was 0.141. The figure illustrates that the Poisson's ratio of 10% FA concrete increased by 39.7%, while those for 15%, 20%, and 25% FA concrete increased by 61.0%, 85.8%, and 103.5%, respectively. This rise may be attributed to the inclusion of FA, which enhances the elastic properties. Noaman et al. [26] stated that the Poisson's ratio increased due to the addition of pozzolanic materials, which improved the elastic properties. Thus, it can be concluded that the Poisson's ratio increases with an increasing FA content in BAC.

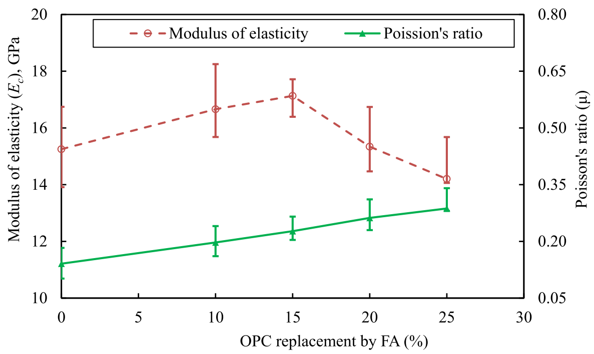

Fig. 7. Modulus of elasticity and Poisson's ratio of FBAC.

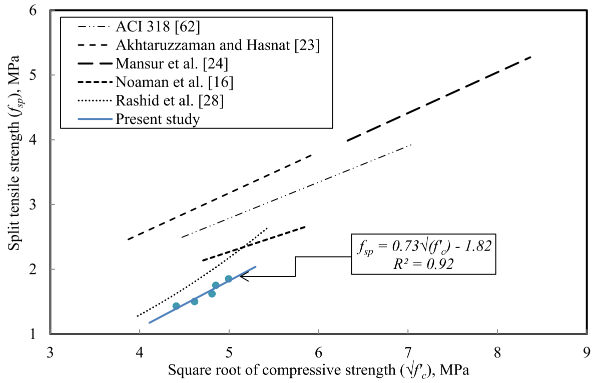

Fig. 8. Relationship between split tensile strength and compressive strength of FBAC.

Table 5
Relationship between compressive strength and other mechanical properties.

Mechanical Properties of concrete	Proposed relation	R^2 value	Reference
Split tensile strength (MPa)	$f_{sp} = 0.56\sqrt{(f_c^{'})}$	0.99	ACI 318 [62]
	$f_{sp} = 0.62\sqrt{(f_c^{'})}$	–	Akhtaruzzaman and Hasnat [23]
	$f_{sp} = 0.63\sqrt{(f_c^{'})}$	–	Mansur et al. [24]
	$f_{sp} = 0.45\sqrt{(f_c^{'})}$	–	Noaman et al. [26]
	$f_{sp} = 0.0514(f_c^{'})^{1.164}$	0.98	Rashid et al. [28]
	$f_{sp} = 0.73\sqrt{(f_c^{'})} - 1.82$	0.92	Present study
Flexural strength (MPa)	$f_r = 0.62\sqrt{(f_c^{'})}$	0.99	ACI 318 [62]
	$f_r = 0.69\sqrt{(f_c^{'})}$	–	Akhtaruzzaman and Hasnat [23]
	$f_r = 0.78\sqrt{(f_c^{'})}$	–	Mansur et al. [24]
	$f_r = 1.04\sqrt{(f_c^{'})}$	–	Noaman et al. [26]
	$f_r = 1.06\sqrt{(f_c^{'})}$	–	Rashid et al. [27]
	$f_r = 1.95\sqrt{(f_c^{'})} - 4.54$	0.78	Present study
Modulus of elasticity (MPa)	$E_c = 4730\sqrt{(f_c^{'})}$	0.99	ACI 318 [62]
	$E_c = 4000\sqrt{(f_c^{'})}$	–	Akhtaruzzaman and Hasnat [23]
	$E_c = 3700\sqrt{(f_c^{'})}$	–	Mansur et al. [24]
	$E_c = 3087.1\sqrt{(f_c^{'})}$	–	Noaman et al. [26]
	$E_c = 3124.5\sqrt{(f_c^{'})}$	–	Rashid et al. [27]
	$E_c = 5324\sqrt{(f_c^{'})} - 12182$	0.92	Rashid et al. [28]
	$E_c = 4009.8\sqrt{(f_c^{'})} - 5168$	0.73	Present study

3.4. Relationship between compressive strength and other mechanical properties

3.4.1. Relationship between f_{sp} and $f_c^{'}$ of FBAC

The relationship between f_{sp} and $f_c^{'}$ of FBAC is shown in Fig. 8. The figure reveals that the f_{sp} of FBAC rises linearly with an increase in $f_c^{'}$. The following equation (Eq. 1) may be used to compute the split tensile strength of FBAC:

$$f_{sp} = 0.73\sqrt{(f_c^{'})} - 1.82 \quad (1)$$

Both the f_{sp} and $f_c^{'}$ values are in MPa. This equation (Eq. 1) has been satisfactorily compared to the earlier researches [23,24,26,28,62] as shown in Table 5. The table reveals that the relations suggested by preceding authors [23,24,26,28,62] are linear equations except Rashid et al. [28]. The authors [28] proposed power formula for calculating tensile strength, whereas the present study shows a best-fit linear equation for FBAC. It is worth noting that the incongruity arose because the authors [23,24,28] recommended this relationship only for BAC, while Noaman et al. [26] proposed it for BAC with rice husk ash. However, ACI 318 [62] presents a relationship between f_{sp} and $f_c^{'}$ of normal-weight concrete. It may be mentioned here that the current analysis provides this relationship (Eq. (1)) only for FBAC at a w/b ratio of 0.50 and a mix proportion of 1:1.5:3.

3.4.2. Relationship between f_r and $f_c^{'}$ of FBAC

Fig. 9 illustrates the relationship between f_r and $f_c^{'}$ of FBAC, indicating that the flexural strength of FBAC increases linearly with the

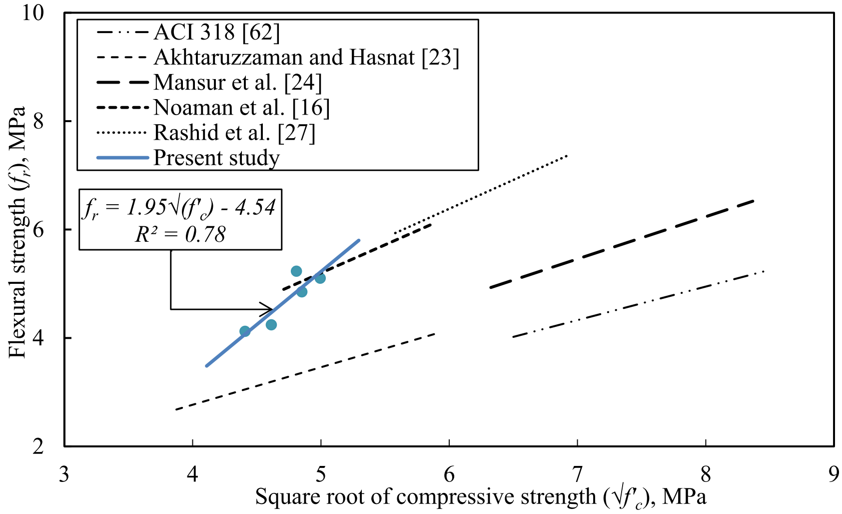

Fig. 9. Relationship between flexural strength and compressive strength of FBAC.

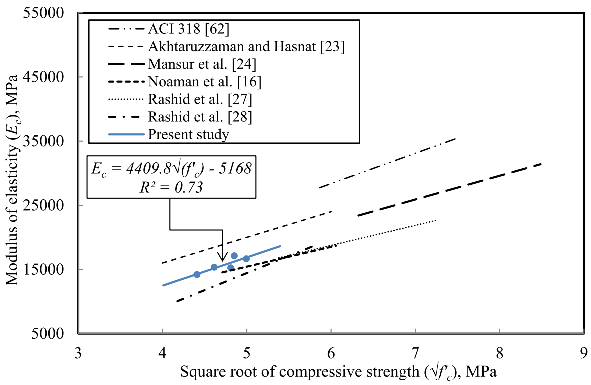

Fig. 10. Relationship between modulus of elasticity and compressive strength of FBAC.

rise in compressive strength. The equation shown below (Eq. (2)) can be used to represent this relationship:

$$f_r = 1.95\sqrt{\left(f_c^{'}\right)} - 4.54 \tag{2}$$

The values of f_r and $f_c^{'}$ are both in MPa. Table 5 provides a comparison of this equation with previous studies [23,24,26,27,62]. The table shows that the correlations proposed by previous authors [23,24,26,27,62] are linear equations. The present study also establishes a best-fit linear relationship for FBAC. The earlier authors [23,24,27] exclusively focused on BAC, whereas Noaman et al. [26] considered BAC with rice husk ash. In addition, a relationship between f_r and square root of $f_c^{'}$ for normal-weight concrete is drawn by ACI 318 [62]. In contrast, the present study offers a novel equation (Eq. 2) mainly for FBAC at a w/b ratio of 0.50 and a mix proportion of 1:1.5:3.

3.4.3. Relationship between $\mathbf{E_c}$ *and* $\mathbf{f_c^{'}}$ *of FBAC*

Fig. 10 illustrates a relationship between the modulus of elasticity (E_c) and compressive strength $\left(f_c^{'}\right)$ of FBAC. According to the figure, E_c went up linearly with the increase of $f_c^{'}$ in FBAC. The equation (Eq. 3) for expressing the E_c of FBAC is as follows:

$$E_c = 4009.8\sqrt{\left(f_c^{'}\right)} - 5168 \tag{3}$$

Both E_c and $f_c^{'}$ values are reported in MPa. In Table 5, this expression is compared with previous research [23,24,26–28,62]. The correlations proposed by previous authors are linear equations and the present study also establishes a best-fit linear relationship for FBAC. The earlier researchers [23,24,27,28] primarily emphasized on BAC without utilizing FA. However, Noaman et al. [26] specially

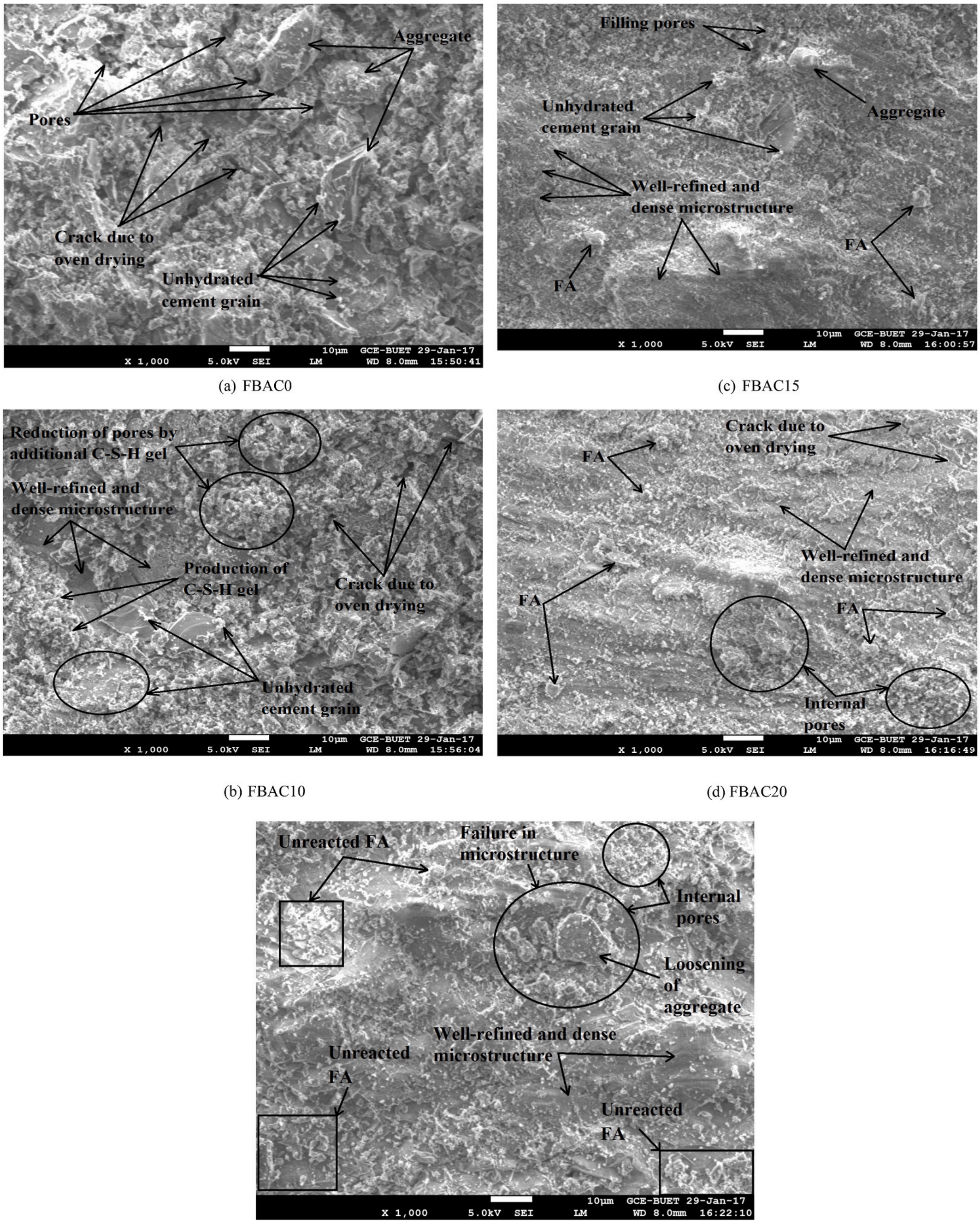

(a) FBAC0 (c) FBAC15

(b) FBAC10 (d) FBAC20

(e) FBAC25

Fig. 11. Microstructure of FBAC after 28 days of curing ((a) FBAC0, (b) FBAC10, (c) FBAC15, (d) FBAC20, and (e) FBAC25).

considered BAC with rice husk ash. Additionally, ACI 318 [62] provides a relationship between E_c and square root of $f_c^{'}$ for normal-weight concrete as shown in Table 5. It may be mentioned here that the present study proposes the relation (Eq. (3)) between E_c and $f_c^{'}$ particularly for FBAC at a w/b ratio of 0.50 and a mix proportion of 1:1.5:3.

3.5. Microstructure of FBAC

Microstructural improvement of BAC containing 0–25% FA at 28 days was explored by SEM investigation (Fig. 11). Fig. 11(a) shows the microstructure of control concrete (0% FA) with enormous number of pores, massive amount of un-hydrated cement grains, and cracks (occurred due to oven dry). However, Fig. 11(b) shows the microstructure of 10% FA concrete with smaller pores, less un-hydrated cement grains, and production of additional C-S-H gel, along with similar cracks due to oven drying compared to Fig. 11(a). On the other hand, Fig. 11(c) displays the microstructure of 15% FA concrete, having negligible pores, very fewer un-hydrated cement grains and well refined and dense microstructure. Fig. 11(b) and (c) also reveal that raw FA improves the microstructure of BAC. These results also indicate that the amount of pores and un-hydrated cement decreases with increase in raw FA. In addition, Fig. 11(d) indicates the microstructure of 20% FA concrete with few amounts of internal pores and spreading of un-reacted FA. Again, Fig. 11(e) illustrates the microstructure of 25% FA concrete with internal pores and many un-reacted FA. This means that an increase in the amount of FA (resulting in an increase in silica contained in FA) reduces an equivalent amount of OPC (reducing the calcium oxide content in OPC) in the concrete. In some places, the inclusion of 25% FA shows loosening of aggregate and consequently failure in the microstructure of BAC. From Fig. 11(a–e), it is clearly seen that the increment of raw FA decreases the voids in BAC due to the pozzolanic and filler effects of FA. A similar observation was also made by Uzbaş and Aydin [10] for FA concrete. The authors [10] stated that the FA (up to 10% replacement) in concrete improved the microstructure of concrete. Papadakis [63] reported that FA improves microstructure of concrete. Thus, it is clear that raw FA in BAC participates in pozzolanic reaction and forms C-S-H gel. Therefore, the raw FA in BAC (up to 15% FA) shows a solid and homogeneous microstructure.

4. Conclusions

In this study, raw FA was incorporated into brick aggregate concrete as a replacement of cement (0–25%). The compressive strengths of hardened FBAC were determined at three curing ages (7, 28 and 90 days) with a w/b ratio of 0.50. Later, the properties of FBAC and its microstructure were investigated at 28 days. The main outcomes of the study are summarized below.

- The FA used in this experiment is Class F pozzolana, characterized by irregular shapes and rough surfaces.
- The workability of fresh FBAC decreases as the raw FA content increases.
- At early ages, the compressive strength of FBAC is lower than control BAC. However, at later ages, this FBAC exhibits higher strength, with 10% FA replacement yielding the maximum compressive strength.
- FBACs demonstrate higher tensile strength (up to 15% replacement) compared to control concrete, and the f_{sp} of FBAC can be calculated using Eq. (1).
- The flexural strength of FBACs exhibited a decrease of 2.5–21.2% compared to that of control concrete, and the f_r of FBAC can be computed using Eq. (2).
- The modulus of elasticity of FBACs (up to 20% replacement) was found to be 0.6–12.3% higher than that of control concrete, with 15% FA replacement demonstrating the highest value, and the E_C of FBAC can be estimated using Eq. (3).
- The Poisson's ratio of FBAC tends to increase as the FA content increases, reaching its peak at a 25% replacement level.
- At 15% FA content, the microstructure of BAC exhibits better characteristics due to both filler and pozzolanic action.

Data availability statement

No additional information is available for this paper.

CRediT authorship contribution statement

Md. Nazrul Islam: Writing – review & editing, Supervision, Conceptualization. **Md. Abu Noaman:** Writing – review & editing, Software, Formal analysis, Conceptualization, Writing – original draft. **Khandaker Saiful Islam:** Writing – original draft, Methodology, Investigation, Data curation. **Mohammad Abu Hanif:** Resources, Investigation, Data curation.

Declaration of competing interest

The authors declare that they have no known competing financial interests or personal relationships that could have appeared to influence the work reported in this paper.

Acknowledgement

The authors would like to extend their heartfelt appreciation to the Department of Civil Engineering of Dhaka University of Engineering & Technology, Gazipur, for their generous financial and technical assistance.

References

[1] A.J. Olarewaju, Engineering properties of concrete mixed with varying degrees of fly ash, Am. J. Eng. Res. (AJER) 5 (9) (2016) 146–149. https://ajer.org/papers/v5(09)/V050901460149.pdf. (Accessed 26 August 2023).
[2] B. Kim, M. Prezzi, Evaluation of the mechanical properties of class-F fly ash, Waste Manag. 28 (3) (2008) 649–659, https://doi.org/10.1016/j.wasman.2007.04.006.
[3] D.K. Nayak, P.P. Abhilash, R. Singh, R. Kumar, V. Kumar, Fly ash for sustainable construction: a review of fly ash concrete and its beneficial use case studies, Cleaner Materials 6 (9) (2022) 100143, https://doi.org/10.1016/j.clema.2022.100143.

[4] Agency, IEA, International Energy, Global Energy Review 2021 – assessing the effects of economic recoveries on global energy demand and CO2 emissions in 2021, Glob. Energy Rev. (2021) 1–36. https://regulator.gov.az/uploads/Beyn%C9%99lxalq%20hesabatlar/GlobalEnergyReview2021.pdf.
[5] F. Birol, Technology Roadmap - Low-Carbon Transition in the Cement Industry, International Energy Agency, 2018. https://www.wbcsd.org/contentwbc/download/4586/61682/1.
[6] G.U. Fayomi, S.E. Mini, O.S.I. Fayomi, A.A. Ayoola, Perspectives on environmental CO2 emission and energy factor in Cement Industry, IOP Conf. Ser. Earth Environ. Sci. 331 (1) (2019) 012035, https://doi.org/10.1088/1755-1315/331/1/012035.
[7] C.T. Jung, K.H. Boon, T.H. Kwong, The effect of fly ash on brick aggregate concrete, Int. J. Civ. Eng. 7 (2) (2020) 19–23, https://doi.org/10.14445/23488352/ijce-v7i2p103.
[8] M.R. Karim, M.F.M. Zain, M. Jamil, F.C. Lai, M.N. Islam, Strength development of mortar and concrete containing fly ash: a review, Int. J. Phys. Sci. 6 (17) (2011) 4137–4153. https://academicjournals.org/journal/IJPS/article-full-text-pdf/7B0536926451.pdf.
[9] T. Meng, D. Dai, X. Yang, H. Yu, Effect of fly ash on the mechanical properties and microstructure of cement-stabilized materials with 100% recycled mixed aggregates, Minerals 11 (9) (2021) 992, https://doi.org/10.3390/min11090992.
[10] B. Uzbaş, A.C. Aydin, Analysis of fly ash concrete with scanning electron microscopy and x-ray diffraction, Adv. Sci. Technol. Res. J. 13 (4) (2019) 100–110, https://doi.org/10.12913/22998624/114178.
[11] M. Zabihi-Samani, S.P. Mokhtari, F. Raji, Effects of fly ash on mechanical properties of concrete, J. Appl. Eng. Sci. 8 (2) (2018) 35–40, https://doi.org/10.2478/jaes-2018-0016.
[12] P.K. Mehta, Properties of blended cements made from rice husk ash, ACI J. Proc. 74 (9) (1977), https://doi.org/10.14359/11022.
[13] G. Li, X. Wu, Influence of fly ash and its mean particle size on certain engineering properties of cement composite mortars, Cement Concr. Res. 35 (6) (2005) 1128–1134, https://doi.org/10.1016/j.cemconres.2004.08.014.
[14] R. Cheerarot, C. Jaturapitakkul, A study of disposed fly ash from landfill to replace Portland cement, Waste Manag. 24 (7) (2004) 701–709, https://doi.org/10.1016/j.wasman.2004.02.003.
[15] H. Toutanji, N. Delatte, S. Aggoun, R. Duval, A. Danson, Effect of supplementary cementitious materials on the compressive strength and durability of short-term cured concrete, Cement Concr. Res. 34 (2) (2004) 311–319, https://doi.org/10.1016/j.cemconres.2003.08.017.
[16] M.A. Noaman, M.R. Karim, M.N. Islam, M.S. Mia, Strength and durability parameters of brick aggregate concrete incorporating rice husk ash as a partial replacement of cement, Adv. Mater. Sci. Eng. 2022 (5) (2022) 1–19, https://doi.org/10.1155/2022/8541276.
[17] M. Adamson, A. Razmjoo, A. Poursaee, Durability of concrete incorporating crushed brick as coarse aggregate, Construct. Build. Mater. 94 (1) (2015) 426–432, https://doi.org/10.1016/j.conbuildmat.2015.07.056.
[18] T. Gupta, K.A. Patel, S. Siddique, R.K. Sharma, S. Chaudhary, Prediction of mechanical properties of rubberised concrete exposed to elevated temperature using ANN, Measurement 147 (12) (2019) 106870, https://doi.org/10.1016/j.measurement.2019.106870.
[19] C. Berryman, J. Zhu, W. Jensen, M. Tadros, High-percentage replacement of cement with fly ash for reinforced concrete pipe, Cement Concr. Res. 35 (6) (2005) 1088–1091, https://doi.org/10.1016/j.cemconres.2004.06.040.
[20] M.D.A. Thomas, Optimizing the Use of Fly Ash in Concrete, Portland Cement Association (PCA), Skokie, Illinois, USA, 2007, pp. 1–24. https://www.cement.org/docs/default-source/fc_concrete_technology/durability/is548-optimizing-the-use-of-fly-ash-in-concrete.pdf.
[21] V.G. Papadakis, S. Tsimas, Supplementary cementing materials in concrete, Cement Concr. Res. 32 (10) (2002) 1525–1532, https://doi.org/10.1016/s0008-8846(02)00827-x.
[22] K.G. Babu, G.S. Nageswara Rao, Efficiency of fly ash in concrete, Cement Concr. Compos. 15 (4) (1993) 223–229, https://doi.org/10.1016/0958-9465(93)90025-5.
[23] A.A. Akhtaruzzaman, A. Hasnat, Properties of concrete using crushed brick as aggregate, Concr. Int. 5 (2) (1983) 58–63. https://www.concrete.org/publications/internationalconcreteabstractsportal/m/details/id/9143. (Accessed 26 August 2023).
[24] M.A. Mansur, T.H. Wee, L.S. Cheran, Crushed bricks as coarse aggregate for concrete, ACI Mater. J. 96 (4) (1999), https://doi.org/10.14359/649.
[25] M.A. Noaman, M.R. Karim, M.N. Islam, Comparative study of pozzolanic and filler effect of rice husk ash on the mechanical properties and microstructure of brick aggregate concrete, Heliyon 5 (6) (2019) e01926, https://doi.org/10.1016/j.heliyon.2019.e01926.
[26] M.A. Noaman, M.N. Islam, M.R. Islam, M.R. Karim, Mechanical properties of brick aggregate concrete containing rice husk ash as a partial replacement of cement, J. Mater. Civ. Eng. 30 (6) (2018), https://doi.org/10.1061/(asce)mt.1943-5533.0002272.
[27] M.A. Rashid, T. Hossain, M.A. Islam, Properties of higher strength concrete made with crushed brick as course aggregate, J. Civ. Eng. 37 (1) (2009) 43–52. https://jce-ieb.org/doc_file/3701004.pdf. (Accessed 27 January 2024).
[28] M.A. Rashid, M.A. Salam, S.K. Shill, M.K. Hasan, Effect of replacing natural coarse aggregate by brick aggregate on the properties of concrete, DUET Inst. Reposit.; DUET J. 1 (3) (2012) 17–22. http://103.133.35.64:8080/xmlui/handle/123456789/357. (Accessed 27 January 2024).
[29] ASTM C29, Test Method for Bulk Density (Unit Weight) and Voids in Aggregate, American Society for Testing and Materials, 1997, https://doi.org/10.1520/c0029_c0029m-97.
[30] ASTM C136, Test Method for Sieve Analysis of Fine and Coarse Aggregates, American Society for Testing and Materials, 2001, https://doi.org/10.1520/c0136-01.
[31] ASTM C127, Test Method for Relative Density (Specific Gravity) and Absorption of Coarse Aggregate, American Society for Testing and Materials, 2001, https://doi.org/10.1520/c0127-01.
[32] ASTM C128, Test Method for Relative Density (Specific Gravity) and Absorption of Fine Aggregate, American Society for Testing and Materials, 2015, https://doi.org/10.1520/c0128-15.
[33] ASTM C566, Test Method for Total Evaporable Moisture Content of Aggregate by Drying, American Society for Testing and Materials, 2013, https://doi.org/10.1520/c0566-13.
[34] ASTM C150, Specification for Portland Cement, American Society for Testing and Materials, 2004, https://doi.org/10.1520/c0150-04.
[35] B. Nanda, S. Rout, Properties of concrete containing fly ash and bottom ash mixture as fine aggregate, Int. J. Sustain. Eng. 14 (4) (2021) 809–819, https://doi.org/10.1080/19397038.2021.1920641.
[36] M. Amin, B.A. Abdelsalam, Efficiency of rice husk ash and fly ash as reactivity materials in sustainable concrete, Sustain. Environ. Res. 29 (1) (2019), https://doi.org/10.1186/s42834-019-0035-2.
[37] A. Durán-Herrera, C.A. Juárez, P. Valdez, D.P. Bentz, Evaluation of sustainable high-volume fly ash concretes, Cement Concr. Compos. 33 (1) (2011) 39–45, https://doi.org/10.1016/j.cemconcomp.2010.09.020.
[38] BS 1377, Determination of Particle Density and Bulk Density of Materials, British Standards, 1990. BS 1377-1390.
[39] ASTM C187, Test Method for Amount of Water Required for Normal Consistency of Hydraulic Cement Paste, American Society for Testing and Materials, 1998, https://doi.org/10.1520/c0187-98.
[40] ASTM C191, Test Methods for Time of Setting of Hydraulic Cement by Vicat Needle, American Society for Testing and Materials, 2001, https://doi.org/10.1520/c0191-01.
[41] ASTM C109, Test method for compressive strength of hydraulic cement mortars (using 2-in. Or [50-mm] Cube Specimens), American Society for Testing and Materials, 2007, https://doi.org/10.1520/c0109_c0109m-07.
[42] ASTM C618, Specification for Coal Fly Ash and Raw or Calcined Natural Pozzolan for Use in Concrete, American Society for Testing and Materials, 2005, https://doi.org/10.1520/c0618-05.
[43] ASTM C143, Test Method for Slump of Hydraulic-Cement Concrete, American Society for Testing and Materials, 2020, https://doi.org/10.1520/c0143_c0143m-20.
[44] ASTM C31, Practice for Making and Curing Concrete Test Specimens in the Field, American Society for Testing and Materials, 2003, https://doi.org/10.1520/c0031_c0031m-03.

[45] ASTM C39, Test Method for Compressive Strength of Cylindrical Concrete Specimens, American Society for Testing and Materials, 2003, https://doi.org/10.1520/c0039_c0039m-03.
[46] ASTM C293, Test Method for Flexural Strength of Concrete (Using Simple Beam with Center-point Loading), American Society for Testing and Materials, 2002, https://doi.org/10.1520/c0293-02.
[47] ASTM C496, Test Method for Splitting Tensile Strength of Cylindrical Concrete Specimens, American Society for Testing and Materials, 2004, https://doi.org/10.1520/c0496_c0496m-04.
[48] ASTM C469, Test Method for Static Modulus of Elasticity and Poissons Ratio of Concrete in Compression, American Society for Testing and Materials, 2002, https://doi.org/10.1520/c0469-02.
[49] Y.H. Mugahed Amran, M.G. Soto, R. Alyousef, M. El-Zeadani, H. Alabduljabbar, V. Aune, Performance investigation of high-proportion Saudi-fly-ash-based concrete, Resul. Eng. 6 (3) (2020) 100118, https://doi.org/10.1016/j.rineng.2020.100118.
[50] G. Yilmaz, Structural characterization of glass–ceramics made from fly ash containing SiO2–Al2O3–Fe2O3–CaO and analysis by FT-IR–XRD–SEM methods, J. Mol. Struct. 1019 (3) (2012) 37–42, https://doi.org/10.1016/j.molstruc.2012.03.028.
[51] T. Fantu, G. Alemayehu, G. Kebede, Y. Abebe, S.K. Selvaraj, V. Paramasivam, Experimental investigation of compressive strength for fly ash on high strength concrete C-55 grade, Mater. Today: Proc. 46 (17) (2021) 7507–7517, https://doi.org/10.1016/j.matpr.2021.01.213.
[52] V. Sata, C. Jaturapitakkul, K. Kiattikomol, Influence of pozzolan from various by-product materials on mechanical properties of high-strength concrete, Construct. Build. Mater. 21 (7) (2007) 1589–1598, https://doi.org/10.1016/j.conbuildmat.2005.09.011.
[53] K. Bazzar, F.Z. Hafiane, A.H. Alaoui, The early age strength improvement of the high volume fly ash mortar, Civil Eng. J. 7 (8) (2021) 1378–1388, https://doi.org/10.28991/cej-2021-03091731.
[54] P. Chindaprasirt, S. Rukzon, Pore structure changes of blended cement pastes containing fly ash, rice husk ash, and palm oil fuel ash caused by carbonation, J. Mater. Civ. Eng. 21 (11) (2009) 666–671.
[55] J. Sun, X. Shen, G. Tan, J.E. Tanner, Compressive strength and hydration characteristics of high-volume fly ash concrete prepared from fly ash, J. Therm. Anal. Calorim. 136 (2) (2018) 565–580, https://doi.org/10.1007/s10973-018-7578-z.
[56] I.B. Muhit, S.S. Ahmed, M.M. Amin, M.T. Raihan, Effects of silica fume and fly ash as partial replacement of cement on water permeability and strength of high performance concrete, in: International Conference on Advances in Civil Engineering, 2013, pp. 108–115. New Delhi, India. DOI: 02.AETACE.2013.4.13.
[57] R. Siddique, Properties of concrete incorporating high volumes of class F fly ash and san fibers, Cement Concr. Res. 34 (1) (2004) 37–42, https://doi.org/10.1016/s0008-8846(03)00192-3.
[58] N. Bouzoubaâ, M.H. Zhang, V.M. Malhotra, Mechanical properties and durability of concrete made with high-volume fly ash blended cements using a coarse fly ash, Cement Concr. Res. 31 (10) (2001) 1393–1402, https://doi.org/10.1016/s0008-8846(01)00592-0.
[59] R. Upadhyay, V. Srivastava, A. Herbert, P.K. Mehta, Effect of fly ash on flexural strength of portland pozzolona cement concrete, J. Academia Industr. Res. (JAIR) 3 (5) (2014) 218–220. http://jairjp.com/OCTOBER%202014/04%20RAHUL.pdf. (Accessed 27 January 2024).
[60] A.M. Neville, Properties of Concrete: Fourth and Final Edition, John Wiley & Sons, 1996.
[61] A.M. Brandt, Cement-Based Composites: Materials, Mechanical Properties and Performance, second ed., CRC Press, 2009.
[62] ACI Committee 318, 318-11: building code requirements for structural concrete and commentary. https://www.concrete.org/publications/internationalconcreteabstractsportal/m/details/id/51683206, 2011.
[63] V.G. Papadakis, Effect of fly ash on Portland cement systems, Cement Concr. Res. 29 (11) (1999) 1727–1736, https://doi.org/10.1016/s0008-8846(99)00153-2.